Proceedings of the 17th World Congress
The International Federation of Automatic Control
Seoul, Korea, July 6-11, 2008

A Novel Approach to Real Time Tire-Road Grip and Slip Monitoring

A. Andrieux * **R. Lengellé** ** **P. Beauseroy** *** **C. Chabanon** ****

* *RENAULT SAS, Guyancourt, 78288 France (Tel: 01-768-50995; e-mail: arnaud.andrieux@renault.com).*
** *ICD-M2S FRE CNRS 2848 University of Technology of Troyes, Troyes, 10010 France (e-mail: regis.lengelle@utt.fr).*
*** *ICD-M2S FRE CNRS 2848 University of Technology of Troyes, Troyes, 10010 France (e-mail: pierre.beauseroy@utt.fr).*
**** *RENAULT SAS, Guyancourt, 78288 France (e-mail: christian.chabanon@renault.com).*

Abstract: It is a very challenging task to measure longitudinal slip of a tire on road surface in normal driving conditions, because of the very small value of the slip (a few 1/1000). This paper presents an industrially deployable method for Tire-Road Friction (TRF) monitoring applied to passenger vehicle. This method estimates the longitudinal wheel slip κ and the normalized friction coefficient μ, for low grip requirement driving conditions, in real time. It uses wheels velocity and forces applied on wheels bearings. Due to the imperfections in the wheel speed sensors used, signal to noise ratio from speed measurement is very low. A correction, taking into account the measured deterministic component of the speed measurement noise (called sensor signature), allows for a correction of wheels speed signals and, accordingly, a better estimation of slip. The obtained results demonstrate the ability of our method to distinguish between wet and dry roads during a longitudinal stabilized drive. This method finds applications in Adaptive Cruise Control systems, Driving Assistance systems and Intelligent Highways.

Keywords: Modeling, supervision, control and diagnosis of automotive systems.

1. INTRODUCTION

According to the report PREDIT (2002), rainy conditions pose tremendous challenges to highways traffic and increase by 72% the risk of accident. The "Etude Detaillée d'Accident" data base from the Biomechanical and Accidentology Laboratory (LAB (2006)) also mentions that 24% of car accidents implying a passenger vehicle take place under degraded adhesion conditions and are observed in straight line. In particular, these statistical data show the bad human perception of TRF level.

Automatic TRF monitoring can contribute to solve this problem. Informations about the actual maximum available grip level can be delivered to the driver, to the vehicle or to the road infrastructure. Real time grip estimation methods are still available (Zami (2005)). Some of them require very specific sensors such as optical speed sensors, dynamometric hubs or gyroscopic measurement systems (Vandanjon et al. (2006)). The costs of these sensors do not allow an industrial implementation. Other approaches use existent sensors (ABS, GPS) and engine models for estimating the longitudinal force (Ray (1997), Carlson and Gerdes (2003)), Lee et al. (2004))). These methods estimate the forces applied to the wheel. Therefore, they require very complex vehicle dynamic and tire models. As it will be shown later, in normal drive conditions, the quantities to be estimated are very small and cannot be distinguished from the model error. Because of this lack of sensibility, these methods are applicable only when high grip is used by the vehicle (braking, for example). Furthermore, the knowledge of the maximum available grip is useful only if it is known before a dangerous situation appears. This is the reason why we consider here the least favourable case: estimating TRF for a vehicle moving at a stabilized speed in straight line, i.e. corresponding to a low grip requirement trajectory. The obtained grip estimate will be used to evaluate the maximum available grip.

The main contribution of this paper is to propose a solution to TRF monitoring that is based on a system that uses only industrial sensors. It is composed of four wheel speed sensors (delivering N pulses per revolution) and four dynamometric wheel bearing sensors set up on a demonstrator. The considered signals for each side of the vehicle are:

- front angular wheel speed ω_f, corresponding to the driving wheel speed
- rear angular wheel speed ω_r
- effective wheel radii R_f and R_r of front and rear wheels respectively
- front longitudinal traction force F_x
- front normal ground reaction force F_z

These signals are used to compute the longitudinal wheel slip κ according to,

$$\begin{aligned} \kappa &= \left(R_f\omega_f - R_r\omega_r\right)/R_f\omega_f \text{ if } F_x > 0 \\ \kappa &= \left(R_r\omega_r - R_f\omega_f\right)/R_r\omega_r \text{ if } F_x < 0 \end{aligned} \quad (1)$$

and the friction coefficient μ,

$$\mu = F_x/F_z. \quad (2)$$

In order to obtain tire-road interaction, we tackle the problem of estimating the coordinates of the measurements in the (μ, κ) space which is often used in the literature, see Pacejka and Bakker (1993), Uchanski (2001), Burckhardt (1987) and Canudas-de-Wit et al. (2003). Figure 1 shows an example of the variation of the friction coefficient μ as a funtion of slip κ for two roadway grip conditions. At a given speed and for given vehicle weight (F_x and F_z are constant), the driving condition corresponds to one value of μ. On figure 1 it can be observed that when the roadway grip conditions change, the value of κ also changes. Therefore, the observed values of μ and κ give us a valuable information on grip conditions and consequently on the maximum available grip μ_{max}. This paper is organized as follow:

- A revue of issues in TRF monitoring for a vehicle moving at stabilized speed in straight line (accuracy of slip measurent, number of measurements, sensor defaults) is presented.
- A methodology for increasing slip measurement accuracy (based on angular wheel speed processing, named *signature correction*) is developed.
- Simulation results are presented and show the possibility to distinguish a dry roadway from a wet roadway.
- A method for determining μ_{max} from (μ, κ) space measurements is finally proposed.

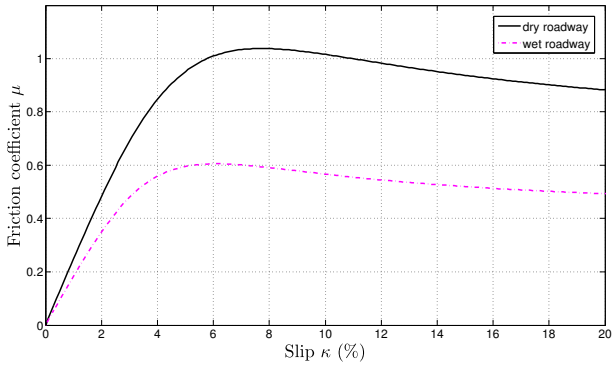

Fig. 1. Example of function $\mu = f(\kappa)$ for two different roadway grip conditions

2. SPEED SIGNALS DENOISING

Table 1 is a summary of Durcos (2006) simulation results. It shows the relation between the values μ and κ corresponding to a stabilized longitudinal drive for different speeds and for a given road having a theorical maximum available friction coefficient μ_{max}. These simulation results have been experimentally confirmed.

Velocity *(km/h)*	μ_{max}	κ (%)	μ
$120km/h$	$1,0$	$0,110$	$0,050$
$120km/h$	$0,8$	$0,140$	$0,050$
$120km/h$	$0,5$	$0,200$	$0,050$
$090km/h$	$1,0$	$0,062$	$0,030$
$090km/h$	$0,8$	$0,080$	$0,030$
$090km/h$	$0,5$	$0,120$	$0,030$
$060km/h$	$1,0$	$0,028$	$0,017$
$060km/h$	$0,8$	$0,036$	$0,017$
$060km/h$	$0,5$	$0,050$	$0,017$
$030km/h$	$1,0$	$0,007$	$0,008$
$030km/h$	$0,8$	$0,009$	$0,008$
$030km/h$	$0,5$	$0,012$	$0,008$

Table 1. Slip and friction coefficient for different speeds and maximum available friction coefficient

As can be seen, the expected sets of data (μ, κ) are very small and close for these driving conditions. They are located close to the origin of the (μ, κ) space. The slip values indicate that obtaining a good slip measurement accuracy requires very accurate wheel speed measurements (see (1)). The next section presents the speed sensors characteristics, observed speed signals and the signal processing method proposed to enhance the signal to noise ratio.

2.1 Origins of the speed sensor noise

The speed sensor performs pulse to pulse timing. Pulses are generated by the movement of magnetic consecutive dipoles in front of a Hall effect sensor. Magnetic dipoles are located on a rim connected to the wheel bearing inner ring. Errors in speed measurements result from:

- the non-uniform repartition of magnetic dipoles
- the eccentricity of the magnetic dipoles repartition (Fig. 2)

Both noise sources present a 1-revolution periodicity and generate a high amplitude deterministic noise component.

Wheel speed is determined according to:

$$V_P = R\left(\theta\left(t_k\right) - \theta\left(t_{k-1}\right)\right)/\left(t_k - t_{k-1}\right), \quad (3)$$

where V_P is the velocity of an arbitrary point P located on the wheel circumference, R is the wheel radius, t_k is the k^{th} pulse time instant and $\theta\left(t_k\right)$ is the angular position of point P at time t_k.

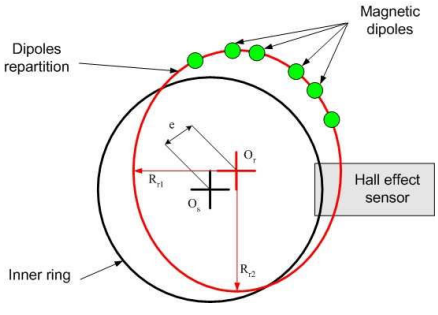

Fig. 2. Geometrical defaults of wheel speed sensor

The method of angular wheel speed noise correction is based on an estimation of the angular localisation of magnetic dipoles over 1-revolution. Thereafter, this localisation is named signature of the wheel speed sensor. In the first step, the signature estimation method is presented and the angular wheel speed signals correction using this signature is introduced.

2.2 Wheel speed sensor signature estimation

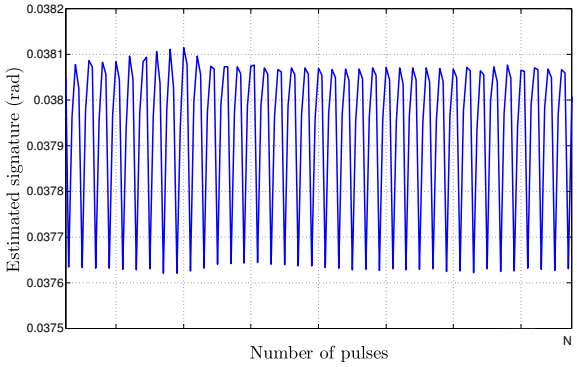

Fig. 3. Example of a signature of a N magnetic dipoles wheel speed sensor

Considering the velocity of the point P as a constant V_0 during the time interval $[0, T]$, the angular deviation $\Delta\theta_k$ between two consecutive pulses can be written:

$$\begin{aligned} V_P(t_k) &= V_0 \quad \forall t_k \in [0, T] \\ \Delta\theta_k &= \theta(t_k) - \theta(t_{k-1}) = V_0(t_k - t_{k-1})/R. \end{aligned} \tag{4}$$

Considering the 1-revolution periodicity of the pulses, $\Delta\theta_k$ values are reproducible from one rotation to the other with a period N corresponding to the number of magnetic dipoles located on the inner ring. Then an estimation of magnetic dipoles angular position error $\widetilde{\Delta\theta_k}$ is determined over m wheel revolutions according to the minimization of:

$$C = \sum_{n=0}^{m-1} \left(\Delta\theta_{k+nN} - \widetilde{\Delta\theta_k}\right)^2. \tag{5}$$

Setting the derivative to 0 gives:

$$\sum_{n=0}^{m-1} \left(\widetilde{\Delta\theta_k}\right) = \sum_{n=0}^{m-1} \left(\Delta\theta_{k+nN}\right). \tag{6}$$

Hence an estimation of the signature $\widetilde{\Delta\theta_k}$, $k = 1 \ldots N$ is obtained:

$$\begin{aligned} \widetilde{\Delta\theta_k} &= \frac{1}{m} \sum_{n=0}^{m-1} \left(\Delta\theta_{k+nN}\right) \\ \widetilde{\Delta\theta_k} &= \frac{1}{m} \sum_{n=0}^{m-1} V_0 \left(t_{k+nN} - t_{k+nN-1}\right). \end{aligned} \tag{7}$$

An example of a wheel speed sensor signature provided with N pulses is represented in (Fig. 3).

2.3 Analysis of the signature variability

Before defining our method for correcting the wheel speed signals, we studied the signature variability in relation to vehicle speed and roadway texture (micro/macro-roughness). Several experiments have been carried out at different speeds (20, 30, 50, 70, 90, 100, 110km/h) and on different kinds of roadway texture (macro-smooth and micro-rough bituminous roadway, macro-rough and micro-rough bituminous roadway, polished concrete and tiling). Figure 4 represents the evolution of the ratio of the quadratic error between the different obtained signatures and an arbitrary chosen reference to the reference signature energy. The reference corresponds to the obtained signature at 20km/h and for a macro-smooth and micro-rough bituminous roadway.

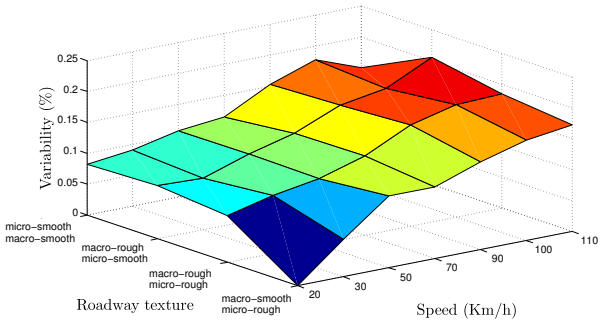

Fig. 4. Signature variability (see text)

According to this criterion, the signature variability ($< 0.2\%$) will be neglected for the rest of this paper. Our denoising method is presented now.

2.4 Wheel speed signals denoising

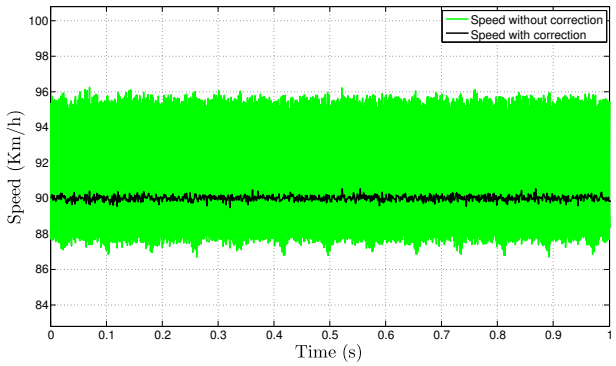

Fig. 5. Example of a speed signal with and without correction

Using the previously estimated wheel speed sensor signature, the angular wheel speed at time t_k is given now by:

$$\omega(t_k) = \widetilde{\Delta\theta_k}/(t_k - t_{k-1}). \tag{8}$$

Finally, the estimated linear speed $\widetilde{V_M}$ of point any M in the contact patch area is given by:

$$\widetilde{V_M}(t_k) = R\widetilde{\Delta\theta_k}/(t_k - t_{k-1}). \quad (9)$$

Figure 5 represents a wheel speed signal with (inner curve) and without (outer curve) signature correction during a stabilized drive at $90km/h$ in straight line. As can be seen the signal to noise ratio is dramatically increased.

Each speed sensor presents its own signature, so this denoising method is applied to each wheel.

3. GRIP MEASUREMENT

Each wheel bearing is also equipped with a dynamic load sensor (SNR. (1995)) that allows a real time preliminary estimation of the load matrix. During a calibration phase, the obtained signals are compared with dynamometric hubs measurements, here considered as a reference, and corrected so as to obtain a satisfactory agreement. A multidimentional nonlinear regression between dynamic load sensors signals and dynamometric hubs mesurements has been performed so as to minimize the prediction error. F_x and F_z are extracted from this corrected load matrix and used to estimate the friction coefficient μ.

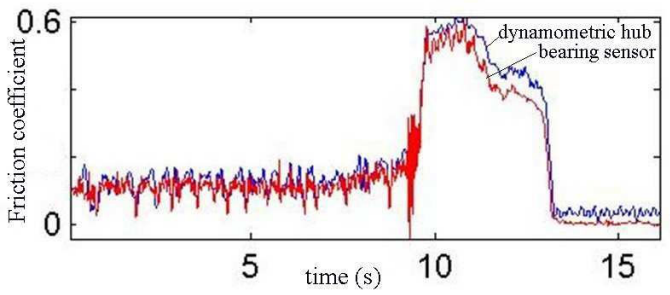

Fig. 6. Example of friction coefficient measurement with dynamometric hub and wheel bearing sensor during a braking maneuver

As shown in figure 6, both measurements of friction coefficient are similar. Differencies in the bandwidths of both sensors can be neglected since, to improve again the signal to noise ratio, all measurements are lowpass filtered as discussed in the next section.

4. REAL TIME MEASUREMENT IN (μ, κ) SPACE

4.1 Slip and grip estimates accuracy enhancement

The presented sensors supply accurate measurements of friction coefficient and slip. To discriminate between different roadway grip conditions and according to simulation results (Tab. 1) the precision of this measurement must be improved. Consequently, an additional lowpass Butterworth filter has been applied on all speed and force signals. The filter cut-off frequency has been selected in accordance with the potential slip variation dynamics and fixed to $1Hz$. As it will be shown later, the filter characteristics act on a compromise between the residual noise amplitude of grip and slip estimates and the delay induced by the filter. This delay will influence the detection delay for a change in roadway grip conditions (see (Fig. 7)).

The upper curves of figure 7 show the unrefined slip estimate as a function of time (outer curve) and the

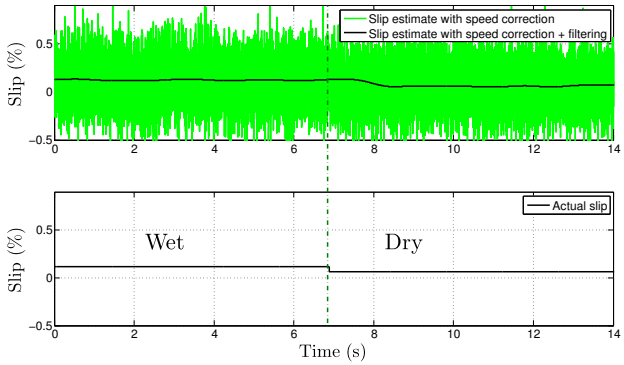

Fig. 7. Example of a change in grip conditions from wet to dry roadway

lowpass filtered estimate (inner curve). The lower curve of figure 7 shows the actual slip variation for a change of μ_{max} from 0.5 to 1.

Using this lowpass filter, we can now evaluate the final precision on the slip estimate by realistic simulations. For a given vehicle speed of $90km/h$ and for every selected value of κ varying within the range $[0.01, 1]\,\%$ we have generated 10000 speed signal realizations of front and rear wheels. Then, an estimate of κ has been calculated for each realization and statistics have been performed. Figure 8 shows the RMS value of the estimation error as a function of the actual κ. Results have been normalized so as to be expressed in percents.

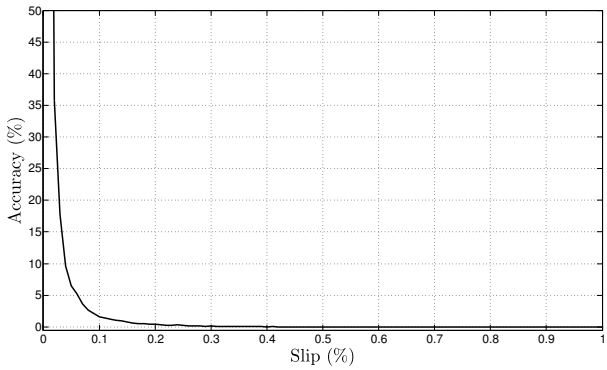

Fig. 8. Normalized RMS κ estimation error as a function of the actual κ

As expected, estimate relative error is a decreasing function of the slip. For a vehicle speed greater than $90km/h$ the slip estimate accuracy can be judged satisfactory (see (Tab. 1) and (Fig. 8)).

4.2 Evaluation of the roadway conditions in (μ, κ) space

For each time instant considered in figure 7, the couple of estimates in the (μ, κ) space can be represented now. On figure 9, the upper subfigure corresponds to the first part of the experiment (wet conditions) and the lower subfigure corresponds to the second part of the experiment (dry conditions), respectively. On both subfigures, loose observations come from the noisy estimates, tight measurements

correspond to the refined estimates. The variance of the estimates are dramatically reduced, so that roadway grip conditions can be easily distinguished, as expected.

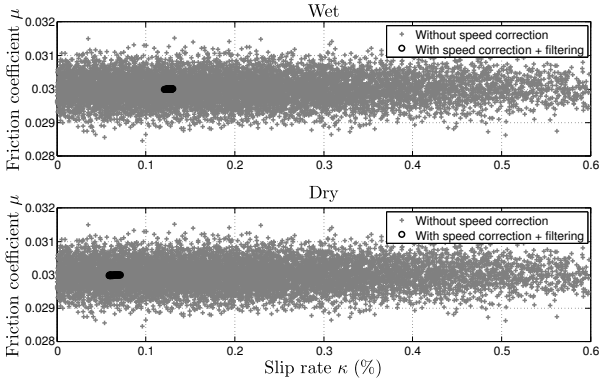

Fig. 9. Representation of the μ and κ estimates in the (μ, κ) space

5. ESTIMATION OF MAXIMUM AVAILABLE FRICTION COEFFICIENT

While the estimation of μ and κ can be efficiently carried out in real time, it is not essential for the driver safety. In case of an emergency, this is not the actual value of μ that will be used, but generally increasing new values of μ up to the maximum available grip corresponding to μ_{max}. So, in terms of safety, determining μ_{max} is a major issue. There are two main methods for estimating μ_{max}.

5.1 Methods based on analytical models $\mu = f(\kappa)$

Many analytical models of the relationship $\mu = f(\kappa)$ can be found in the literature: Pacejka and Bakker (1993), Van Oosten and Bakker (1993), Uchanski (2001), Zami (2005) and Canudas-de-Wit et al. (2003). Models are chosen *a priori* to fit a large class of experimental observations. Identification of the models parameters generally relies on the optimization of a cost function of the model output and observed data. In our study, identification of any model's parameters cannot be performed because, in a low grip requirement trajectory, actual grip and slip measurements are located close to the origin and do not allow an accurate estimation of the model parameters.

5.2 Phenomenologic approach

Another method (Gustafsson (1997)) uses the observed correlation between μ_{max} and the slope λ of the curve $\mu = f(\kappa)$ at the origin. This correlation was confirmed in Uchanski (2001). An estimate of the slope λ is obtained using a Kalman filter. Grip conditions change induces a modification of the slope λ. Detection of such changes can be achieved with a real time detection algorithm like CUSUM, see Basseville and Nikiforov (1991). This method is presented now.

For small values of μ and κ, the relation $\mu = f(\kappa)$ is approximately linear:

$$\mu = \lambda(\kappa - \delta) \tag{10}$$

where δ is a constant representing the wheel radius variation. This equation is preferably written:

$$\kappa = \mu\frac{1}{\lambda} + \delta \tag{11}$$

Considering an additive zero mean white noise $\mathcal{N}_\kappa$, the observation equation becomes:

$$\begin{aligned}\kappa(t) &= \mu(t)\frac{1}{\lambda} + \delta + \mathcal{N}_\kappa \\ &= [\mu(t)\ \ 1]\begin{bmatrix}1/\lambda \\ \delta\end{bmatrix} + \mathcal{N}_\kappa \\ &= H(t)\,\mathbf{x} + \mathcal{N}_\kappa\end{aligned} \tag{12}$$

where $\mathbf{x}$ is the unknown and $H(t) = [\mu(t)\ \ 1]$.

Adding the state equation (corresponding to a stationary grip condition) to the model gives:

$$\begin{aligned}\mathbf{x}(t+1) &= \mathbf{x}(t) + \mathcal{N}_x \\ \kappa(t) &= H(t)\,\mathbf{x}(t) + \mathcal{N}_\kappa\end{aligned} \tag{13}$$

Considering these equations for the left and right sides of the vehicle leads to:

$$\begin{aligned}\kappa(t) &= \begin{bmatrix}\kappa_{left}(t) \\ \kappa_{right}(t)\end{bmatrix} \\ H(t) &= \begin{bmatrix}\mu_{left}(t) & 0 & 1 & 0 \\ 0 & \mu_{right}(t) & 0 & 1\end{bmatrix} \\ \mathbf{x}(t) &= \begin{bmatrix}\dfrac{1}{\lambda_{left}(t)} & \dfrac{1}{\lambda_{right}(t)} & \delta_{left}(t) & \delta_{right}(t)\end{bmatrix}^{\mathsf{T}}\end{aligned} \tag{14}$$

Finally, Kalman equations are iterated to recursively estimate $\mathbf{x}$:

$$\begin{aligned}S(t) &= P(t-1) + Q(t-1) \\ K(t) &= S(t)\,H^{\mathsf{T}}(t)\left(H(t)\,S(t)\,H^{\mathsf{T}}(t) + R(t)\right)^{-1} \\ \hat{\mathbf{x}}(t) &= \hat{\mathbf{x}}(t-1) + K(t)\left(\kappa(t) - H(t)\,\hat{\mathbf{x}}(t-1)\right) \\ P(t) &= S(t) - K(t)\,H(t)\,S(t)\end{aligned} \tag{15}$$

where

$$\begin{aligned}Q(t) &= E\left\{\mathcal{N}_x\mathcal{N}_x^{\mathsf{T}}\right\} \\ R(t) &= E\left\{\mathcal{N}_y\mathcal{N}_y^{\mathsf{T}}\right\}\end{aligned} \tag{16}$$

The noise covariance matrices are unknown. Selecting them leads to a compromise between fast convergence and stability of the estimate. Stability is preferred until a change in grip conditions is detected. In such a case, $Q(t)$ is re-initialized to a value that ensures fast convergence, otherwise $Q(t)$ is iteratively decreased (if it has not reached a fixed minimum value) to improve stability.

The precision obtained by applying our method allows us to discriminate different road grip conditions (such as wet-dry). Investigations are done in order to characterize the relationship $\mu_{max} = g(\lambda)$ in a probabilistic way. Another solution, which is also under investigation, is to use the invariance relationship (17) proposed in Michelin (2002).

$$\mu_{max} = f(\kappa_{opt})$$
$$\left(\frac{\mu_{max}}{\kappa_{opt}}\right) / \left(\frac{\mu(\kappa_{opt}/2)}{\kappa_{opt}/2}\right) = Inv = 0,58 \quad (17)$$

where κ_{opt} is the observed slip value for $\mu = \mu_{max}$.

Here again, the necessary extension of this relation to much closer to the origin κ values must be addressed in a further work.

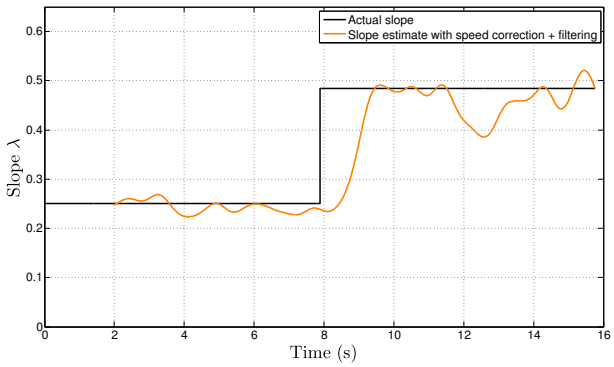

Fig. 10. Exemple of change in slope λ from wet to dry roadway

6. CONCLUSION

In this paper, the problem of real time estimation of tire-road grip and slip of a passenger vehicle in straight line and normal driving conditions has been addressed. Within these driving conditions,we recalled that the slip must be estimated with a very high accuracy. We have presented an industrially deployable measurement system that mainly relies on instrumented wheel bearings and allows joint estimation of slip and grip. We have explained why slip and grip are both necessary to characterize the road grip conditions. A method has been proposed to reduce dramatically the noise on speed signals and thus to improve slip measurements accuracy. Despite the high improvement in signal to noise ratio, additional lowpass filtering of speed and grip signals has been judged necessary. Our work allows the determination of slip with an accuracy of a few 1/1000.

Realistic simulations were performed for a dry and a wet roadway during straight line stabilized drive at $90km/h$. Simulation results have been given in the (μ, κ) space, used as a reference in TRF monitoring. They have shown that it was possible to distinguish these two roadway grip conditions.

For safety purposes, the useful information to the driver is the maximum available friction coefficient μ_{max} rather than the actual friction coefficient μ. The obtained estimates μ and κ have been used for μ_{max} estimation according to a method detailed in Gustafsson (1997) and based on a Kalman filter. This method uses a probabilistic relation between the value of μ_{max} and the slope of the $\mu = f(\kappa)$ curve at the origin. Another approach, based on the *Michelin* patent is under investigation.

ACKNOWLEDGEMENTS

This work was supported by RENAULT SAS.

REFERENCES

M. Basseville and I.V. Nikiforov. A unified framework for statistical change detection. *Proceedings of the IEEE Conference on Decision and Control*, 3:2586 – 2591, 1991. ISSN 0191-2216.

M. Burckhardt. ABS und ASR, sicherheitsrelevantes, radschlupf-regel systeme. Technical report, University of Braunschweig, Germany, 1987.

C. Canudas-de-Wit, P. Tsiotras, E. Velenis, M. Basset, and G. Gissinger. Dynamic friction models for road/tire longitudinal interaction. *Vehicle System Dynamics*, 39 (3):189 – 226, 2003. ISSN 0042-3114.

C.R. Carlson and J.C. Gerdes. Nonlinear estimation of longitudinal tire slip under several driving conditions. *Proceedings of the American Control Conference*, 6:4975 – 4980, 2003. ISSN 0743-1619.

S. Durcos. *Conception d'un système embarqué en vue d'estimer l'adhérence longitudinale*. PhD thesis, Université de Technologie de Troyes, Décembre 2006.

F. Gustafsson. Slip-based tire-road friction estimation. *Automatica*, 33(6):1087 – 1099, 1997. ISSN 0005-1098.

LAB. Etude détaillée d'accidents. Technical report, 2006.

C. Lee, K. Hedrick, and K. Yi. Real-time slip-based estimation of maximum tire-road friction coefficient. *IEEE/ASME Transactions on mechatronics*, 9:454–458, June 2004. ISSN 1083-4435.

Michelin. Brevet FR2842910 Méthode d'asservissement, utilisable pour maintenir le glissement d'un pneu à niveau optimal pour qu'il fonctionne à un niveau de coefficient d'adhérence maximale. Technical report, Société de Technologie Michelin, Juillet 2002.

H.B. Pacejka and E. Bakker. Magic formula tyre model. *Vehicle System Dynamics*, 21(SUPPL):1 – 18, 1993. ISSN 0042-3114.

PREDIT. Accidents par temps de pluie. Technical report, CETE Normandie, Mai 2002.

L. Ray. Nonlinear tire force estimation and road friction identification: simulation and experiments. *Automatica*, 33(10):1087 – 1099, October 1997.

SNR. Brevet FR2736979 Détecteur dynamométrique pour roulements et paliers. Technical report, Juillet 1995.

M.R. Uchanski. *Road Friction Estimation for Automobiles Using Digital Signal Processing Methods*. PhD thesis, University of California, Berkeley, 2001.

J.J.M. Van Oosten and E. Bakker. Determination of magic tyre model parameters. *Vehicle System Dynamics*, 21 (SUPPL):19 – 29, 1993. ISSN 0042-3114.

P.O. Vandanjon, M.T. Do, Y. Delanne, Andrieux. A, and P. Daburon. Comparison of different systems of measurement of skid resistance. *Proceedings of the FISITA World Automotive Congress, Yokohama, Japan*, October 2006.

B. Zami. *Contribution à l'identification de la liaison véhicule-sol d'un véhicule automobile. Estimation des paramètres de modèles de pneumatique*. PhD thesis, Université de Haute Alsace, Mulhouse, Janvier 2005.